Flux penetration in a thin superconducting disk

Alexander L. Fetter
Stanford University, Institute of Theoretical Physics, Physics Department, Stanford, California 94305
(Received 11 February 1980)

Pearl's description of a quantized flux line in an infinite thin superconducting film with an effective penetration depth Λ is generalized to a thin finite disk of radius R. The presence of the boundary precludes an exact analytic solution; instead, the problem is reduced to an integral equation. An approximate solution provides a convenient interpolation between a neutral superfluid film ($R \ll \Lambda$) and an unbounded superconducting film ($R \gg \Lambda$). The lower critical field H_{c1} and the interaction function between two flux lines are evaluated as functions of R/Λ. In the limit of many flux lines with nonoverlapping cores, the flux density is shown to be uniform for arbitrary R/Λ.

I. INTRODUCTION

Recent studies[1-4] of thin superconducting films have led to renewed interest in the detailed structure of flux lines in such geometries. For an infinite film of thickness d and penetration depth λ, Pearl's original calculation[5,6] showed that the interaction energy is logarithmic for $r \lesssim \Lambda = 2\lambda^2/d$ but changes to an inverse dependence for $r \gtrsim \Lambda$. This behavior should be compared with that in a bulk superconductor, where the interaction is logarithmic for $r < \lambda$ but becomes exponentially small for $r \gg \lambda$. Evidently, Λ may be considered an effective penetration depth for a film. The principal difference between a thin film and bulk material is the long-range tail of the interaction in a film. It arises from the overlap of the fringing magnetic fields in the surrounding vacuum and is wholly absent in a bulk superconductor.

For a very thin film, Λ itself can become macroscopically large. This possibility has led to the suggestion that the interaction function in a bounded film with finite transverse dimensions R might be approximately logarithmic for all separations[1-4] if $R \lesssim \Lambda$. Since two-dimensional systems interacting with logarithmic potentials are believed to exhibit special and unusual properties,[7-11] such a situation would be extremely interesting. To provide a basis for detailed study of these problems, the present work considers the structure of a single quantized flux line in a thin superconducting disk of radius R and the corresponding interaction between pairs of such flux lines. In the limit $R \ll \Lambda$, the circulating current has the r^{-1} dependence of a rectilinear vortex line because the superconducting screening effects are negligible. For $R \gg \Lambda$, screening becomes significant in the region $\Lambda \lesssim r \lesssim R$, and, as $R/\Lambda \to \infty$, this screening completely cancels the original r^{-1} vortex flow, leaving Pearl's asymptotic r^{-2} dependence. Correspondingly, the interaction between two such flux lines is approximately logarithmic in a small film ($R \ll \Lambda$). For large R/Λ, however, the interaction changes from logarithmic to r^{-1} for $\Lambda \lesssim r \lesssim R$, and our results reproduce Pearl's as $R/\Lambda \to \infty$. This behavior implies that observable physical quantities like the lower critical field H_{c1} depend significantly on the ratio R/Λ. Thus direct measurements of H_{c1} could help confirm the validity of Pearl's basic picture.

The problem of a quantized flux line at the center of a disk is formulated in Sec. II and reduced to a one-dimensional Fredholm integral equation. In Sec. III, an exact formal solution is constructed, but its form makes direct quantitative calculations cumbersome. Section IV derives an alternative approximate solution that readily yields numerical values for various quantities of physical interest. The more complicated problem of interacting flux lines in arbitrary positions is studied in Sec. V.

II. BASIC FORMULATION

Consider a disk-shaped superconducting film of thickness d and radius R lying in the xy plane. It is natural to introduce cylindrical coordinates (r,θ,z) centered on the disk's symmetry axis. In general, the Ginzburg-Landau equations involve both the superconducting order parameter ψ and the vector potential $\vec{A}$, but we shall neglect the spatial variation of $|\psi|$ and write $\psi = |\psi_0| \exp(iS)$. In this case, the Ginzburg-Landau equations become[5,6,12,13]

$$\vec{\nabla} \times \vec{\nabla} \times \vec{A} = \begin{cases} 4\pi \vec{j}/c & \text{for } |z| < \frac{1}{2}d \text{ and } r < R \\ 0 & \text{otherwise} \end{cases} \tag{1}$$

and

$$\frac{4\pi}{c}\vec{j} = \frac{1}{\lambda^2}\left(\frac{\phi_0}{2\pi}\vec{\nabla}S - \vec{A}\right) , \tag{2}$$

where λ is the actual penetration depth in the film and ϕ_0 is the flux quantum $hc/2e$. Since d/λ is assumed small, $\vec{j}$ and $\vec{A}$ are constant across the film and Eqs. (1) and (2) can be averaged over the thickness d to give

$$\vec{\nabla}\times\vec{\nabla}\times\vec{A}=\frac{d}{\lambda^2}\delta(z)\left(\frac{\phi_0}{2\pi}\vec{\nabla}S-\vec{A}\right)\eta(R-r) \ , \quad (3)$$

where $\eta(x)$ is the usual unit step function. In the special case of a single flux line at the center of the disk, the phase S is just the azimuthal angle θ. The axisymmetry of the problem then implies that $\vec{A}$ is purely azimuthal with the form $\vec{A}=\hat{\theta}A$, where A satisfies the linear differential equation

$$\left(\frac{\partial^2}{\partial z^2}+\frac{\partial^2}{\partial r^2}+\frac{1}{r}\frac{\partial}{\partial r}-\frac{1}{r^2}\right)A = \frac{2}{\Lambda}\delta(z)\left(A-\frac{\phi_0}{2\pi r}\right)\eta(R-r) \ , \quad (4)$$

and

$$\Lambda\equiv 2\lambda^2/d \quad (5a)$$

will play the role of an effective penetration depth. This definition agrees with that of Pearl,[5,6] but some authors[1,2] define

$$\lambda_\perp\equiv\lambda^2/d=\tfrac{1}{2}\Lambda \ , \quad (5b)$$

which differs by a factor of 2. It is convenient to measure lengths in units of R, and A in units of $\phi_0/2\pi R$. These dimensionless variables reduce Eq. (4) to

$$\left(\frac{\partial^2}{\partial y^2}+\frac{\partial^2}{\partial x^2}+\frac{1}{x}\frac{\partial}{\partial x}-\frac{1}{x^2}\right)A(x,y) = \frac{2R}{\Lambda}\delta(y)\left(A-\frac{1}{x}\right)\eta(1-x) \ , \quad (6)$$

where, for clarity, we have introduced the explicitly dimensionless variables $x=r/R$ and $y=z/R$. This is the fundamental inhomogeneous differential equation; it must be solved throughout all space.

Given $A(x)\equiv A(x,0)$, several quantities of physical interest can be found. The first is the total azimuthal supercurrent density

$$j=(c\phi_0/4\pi^2\Lambda R d)\hat{j} \ , \quad (7a)$$

where

$$\hat{j}(x)=x^{-1}-A(x) \ . \quad (7b)$$

Here, dimensionless quantities like $\hat{j}$ will be denoted by a caret, although it will be omitted on A to avoid a cluttered notation for its Hankel transform. The second term of $\hat{j}$ has a direct physical interpretation as the screening current induced by the circulating x^{-1} flow of the quantized vortex. The interaction energy to bring another parallel flux line in from the boundary of the disk to a point x follows by integrating[6] the Lorentz force $(\phi_0 d/c)\vec{j}\times\hat{z}$:

$$U=(\phi_0^2/4\pi^2\Lambda)\hat{U}(x) \ , \quad (8a)$$

where

$$\hat{U}(x)=\ln\frac{1}{x}-\int_x^1 dx'\,A(x') \ , \quad (8b)$$

and the additive constant has been chosen to fix $\hat{U}(1)=0$. Since the first term represents the interaction of two unscreened vortex lines, it is convenient to write

$$\hat{U}(x)=\ln\frac{1}{x}+\hat{U}_{sc}(x) \ , \quad (9a)$$

where

$$\hat{U}_{sc}(x)=-\int_x^1 dx'\,A(x') \quad (9b)$$

characterizes the attractive effect of the screening currents (sc).

The self-energy ϵ of a single flux line located at the origin is the sum of the kinetic energy of the flow and the magnetic field energy. A straightforward calculation using Eqs. (1) and (2) yields the simple answer[6]

$$\epsilon=(\phi_0^2/4\pi^2\Lambda)\hat{\epsilon} \ , \quad (10a)$$

where

$$\hat{\epsilon}=\tfrac{1}{2}\hat{U}(r_c/R) \approx \tfrac{1}{2}\ln(R/r_c)+\tfrac{1}{2}\hat{U}_{sc}(0) \ , \quad (10b)$$

and r_c is the (small) core radius of the flux line. Typical values are $R\approx 10^{-1}$ cm and $r_c\approx 10^{-6}$ cm, so that the first term of $\hat{\epsilon}$ is of order 6.

The total circulating supercurrent produces an associated magnetic moment

$$\vec{m}=(2c)^{-1}\int d^3\vec{r}\,\vec{r}\times\vec{j} \ . \quad (11)$$

It lies along the symmetry axis with magnitude

$$m=(\phi_0 R/2\pi^2)\hat{m} \ , \quad (12a)$$

where

$$\hat{m}=\frac{\pi R}{2\Lambda}\int_0^1 x dx\,[1-xA(x)] \ . \quad (12b)$$

The critical field H_{c1} for flux penetration into the disk is just the ratio of these quantities ϵ/m. Use of Eqs. (10) and (12) gives

$$H_{c1}=(\phi_0/2R\Lambda)\hat{H}_{c1} \ , \quad (13a)$$

where

$$\hat{H}_{c1}=\hat{\epsilon}/\hat{m} \ . \quad (13b)$$

The quantity $\phi_0/2R\Lambda$ is $\approx 10^{-5}$ G for $R=\Lambda=10^{-1}$ cm, but $\hat{H}_{c1}$ can become large for small R/Λ. One of the principal aims of this work is to evaluate these dimensionless functions for various values of R/Λ. In the limit of small R/Λ, they are expected to reproduce those for a bounded neutral superfluid film, whereas for large R/Λ, they should become those for an infinite plane superconducting film.

To derive an integral equation for $A(x)\equiv A(x,0)$, we first take the Hankel transform of Eq. (6) according to

$$\bar{A}(p,y)\equiv\int_0^\infty x\,dx\,J_1(px)A(x,y)\ , \tag{14}$$

where $J_n(px)$ is the Bessel function[14] of order n. Carrying out the indicated operation yields

$$\left(\frac{\partial^2}{\partial y^2}-p^2\right)\bar{A}(p,y)$$
$$=\frac{2R}{\Lambda}\delta(y)\int_0^1 x\,dx\,J_1(px)[A(x)-x^{-1}]$$
$$=\frac{2R}{\Lambda}\delta(y)\left[\int_0^1 x\,dx\,J_1(px)A(x)-p^{-1}[1-J_0(p)]\right]\ . \tag{15}$$

Note that the integral on the right-hand side is over a *finite* interval and therefore differs from the Hankel transform $\bar{A}(p,0)$. It is evident from Eq. (15) that $\bar{A}(p,y)$ for $y\neq 0$ must have the form $A(p)\exp(-p|y|)$, where $\bar{A}(p)$ is a function only of p. It can be determined by integrating Eq. (15) over an infinitesimal region around $y=0$, which gives the condition

$$-2p\bar{A}(p)=\frac{2R}{\Lambda}\left[\int_0^1 x\,dx\,J_1(px)A(x)-p^{-1}[1-J_0(p)]\right]\ . \tag{16}$$

The Hankel inversion theorem then yields a formal expression for the vector potential throughout all space

$$A(x,y)=\int_0^\infty p\,dp\,\bar{A}(p)J_1(px)\exp(-p|y|)\ . \tag{17}$$

It assumes a particularly simple form for $y=0$; a little manipulation leads to the exact integral equation

$$A(x)+\frac{R}{\Lambda}\int_0^1 x'dx'\,L(x,x')A(x')=\frac{R}{\Lambda}\int_0^1 dx'\,L(x,x')\ , \tag{18}$$

with the kernel

$$L(x,x')\equiv\int_0^\infty dp\,J_1(px)J_1(px')\ . \tag{19}$$

This integral equation needs to be solved only for $0\leq x\leq 1$, because substitution of the solution into Eq. (18) in fact determines $A(x)$ for all positive x. The Hankel transform of the resulting function then gives $\bar{A}(p)$, yielding the vector potential throughout all space by Eq. (17). Thus the problem has been reduced to one of solving the linear integral equation (18).

To proceed further, it is helpful to note several of its properties:

(i) The kernel $L(x,x')$ is manifestly symmetric, and the extra weight factor x' can be symmetrized[15] by introducing suitable factors of $x^{1/2}$ and $x'^{1/2}$. Consequently, the problem becomes an inhomogeneous integral equation of the second kind with a real symmetric kernel.

(ii) The integral in Eq. (19) can be transformed by writing $J_1(px_<)J_1(px_>)$ as

$$\tfrac{1}{2}J_1(px_<)[H_1^{(1)}(px_>)+H_1^{(2)}(px_>)]\ ,$$

where $x_<$ and $x_>$ are the smaller and larger of x and x', and $H_1^{(i)}$ are the Hankel functions.[14] A deformation of the integration contour from the real to the (positive or negative) imaginary axis gives the alternative representation

$$L(x,x')=\frac{2}{\pi}\int_0^\infty dp\,I_1(px_<)K_1(px_>)\ , \tag{20}$$

where I_1 and K_1 are the Bessel functions[14] of imaginary argument. Since these functions are positive, Eq. (20) shows that $L(x,x')$ can never be negative. It is not a continuous kernel, however, because the asymptotic behavior $I_1(x)K_1(x)\sim(2x)^{-1}$ for $x\to\infty$ implies that $L(x,x')$ diverges logarithmically as $|x-x'|\to 0$. On the other hand, the kernel is square integrable, for the double integral

$$\mathrm{Tr}L^2\equiv\int\int_0^1 x\,dx\,x'dx'L(x,x')L(x',x) \tag{21}$$

is finite.

(iii) These properties[15] imply that the kernel $L(x,x')$ has an infinite sequence of real eigenvalues l_n and orthornormal eigenfunctions $\psi_n(x)$ satisfying the equations

$$\psi_n(x)=l_n\int_0^1 x'dx'\,L(x,x')\psi_n(x')\ , \tag{22a}$$

$$\int_0^1 x\,dx\,\psi_n(x)\psi_{n'}(x)=\delta_{nn'}\ . \tag{22b}$$

Furthermore, L itself has the form

$$L(x,x')=\sum_{n=1}^\infty l_n^{-1}\psi_n(x)\psi_n(x')\ . \tag{23a}$$

Since $\mathrm{Tr}L^2$ in Eq. (21) is finite, the series

$$\mathrm{Tr}L^2=\sum_{n=1}^\infty l_n^{-2} \tag{23b}$$

converges, but the logarithmic behavior of $L(x,x')$

for $x \to x'$ suggests that l_n increases linearly with n for $n \to \infty$.

(iv) These (still unknown) eigenfunctions provide a formal solution to the integral equation (18). Expand $A(x)$ in this complete set and use the orthonormality to determine the coefficients. A simple calculation yields the result

$$A(x) = \sum_{n=1}^{\infty} \frac{\psi_n(x)}{1 + l_n \Lambda / R} \int_0^1 dx' \, \psi_n(x') \ . \tag{24}$$

This expression shows that $A(x)$ is a meromorphic function of R/Λ, and that the iterated (Neumann) expansion of Eq. (18) in powers of R/Λ converges for $|R/\Lambda| < l_1$. Since $\mathrm{Tr}\, L^2 \geq l_1^{-2}$, convergence is assured for $|R/\Lambda| < (\mathrm{Tr} L^2)^{-1/2}$.

(v) The integral Eqs. (19) and (20) can be evaluated explicitly to give[16]

$$L(x,x') = \frac{2}{\pi x_<} \left[K\left(\frac{x_<}{x_>}\right) - E\left(\frac{x_<}{x_>}\right) \right] \ , \tag{25}$$

where K and E are the complete elliptic integrals of the first and second kind. Since $K(k)$ diverges logarithmically as $k \to 1$, this expression confirms the singularity of the kernel at $x = x'$. Detailed examination shows that $L(0,x') = 0$ and that $L(1,x')$ is finite. Figure 1 shows the function $L(x,x')$ for the typical value $x' = \frac{1}{2}$. The representation Eq. (25) is particularly useful for evaluating the double integral in Eq. (21); a straightforward calculation gives

$$\mathrm{Tr} L^2 = \frac{4}{\pi^2} \int_0^1 \frac{dk}{k} [K(k) - E(k)]^2 \approx 0.237 \ , \tag{26}$$

where the last value follows from numerical integration. Thus the expansion of the solution to Eq. (18) in powers of R/Λ is guaranteed to converge for $R/\Lambda < 2.05$.

(vi) The formal solution Eq. (24) may be used to express the important physical quantities in terms of the exact eigenfunctions, but the resulting formulas for (say) H_{c1} are not terribly useful. Similar expressions will be considered in Sec. IV in connection with an approximate solution based on known eigenfunctions.

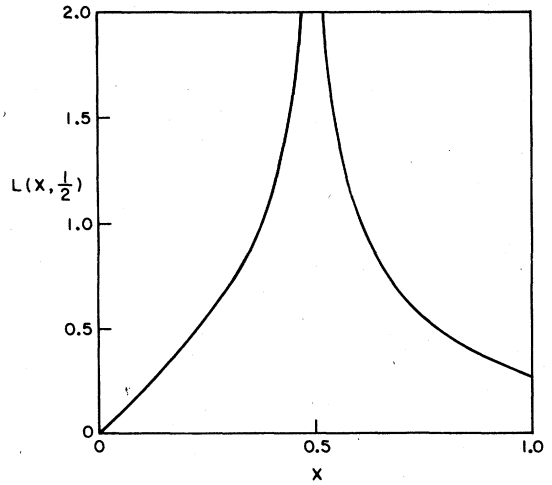

FIG. 1. Real symmetric kernel $L(x,x')$ [Eq. (25)] for $x' = \frac{1}{2}$.

III. EXACT RESULTS

For $R/\Lambda \ll 1$, the screening currents are expected to be small, so that the vector potential A will be well represented by the first term in the Neumann expansion of Eq. (18)

$$A(x) \approx \frac{R}{\Lambda} \int_0^1 dx' \, L(x,x'), \quad R \ll \Lambda \ . \tag{27}$$

An exact evaluation gives[16]

$$A(x) \approx \frac{R}{\Lambda} \left[1 - \frac{2}{\pi x} [E(x) - (1-x^2) K(x)] \right] \ , \quad R \ll \Lambda \ , \tag{28}$$

and substitution into Eq. (9) yields the lowest-order screening contribution to the interaction function

$$\hat{U}_{sc}(x) \approx \frac{R}{\Lambda} \left[x - 1 - \frac{2}{\pi} [2E(x) - 2 - (1-x^2) K(x)] \right] \ , \quad R \ll \Lambda \ . \tag{29}$$

Figure 2 sketches the function in braces, which varies smoothly. Note that Eqs. (28) and (29) both remain finite at $x = 1$ owing to the factor $1 - x^2$ multiplying the singular function $K(x)$. In addition, Eqs. (10b) and (29) provide the approximate expression for the self-energy of a single flux line at the center of a small disk with $R \ll \Lambda$

$$\hat{\epsilon} \approx \tfrac{1}{2} \ln(R/r_c) - (R/\Lambda)(1 - 2\pi^{-1})$$
$$\approx \tfrac{1}{2} \ln(R/r_c) - 0.363 R/\Lambda, \quad R \ll \Lambda \ . \tag{30}$$

Similarly, Eq. (12b) gives the corresponding magnetic moment

$$\hat{m} \approx \frac{\pi R}{4\Lambda} - \left(\frac{R}{\Lambda}\right)^2 \left(\tfrac{1}{6}\pi - \tfrac{2}{9}\right)$$
$$\approx \frac{\pi R}{4\Lambda} \left[1 - 0.384 \frac{R}{\Lambda} \right], \quad R \ll \Lambda \ , \tag{31}$$

and H_{c1} is the ratio of these quantities

$$\hat{H}_{c1} \approx \frac{2\Lambda}{\pi R} \frac{\ln(R/r_c) - 0.727 R/\Lambda}{1 - 0.384 R/\Lambda}, \quad R \ll \Lambda \ . \tag{32}$$

As $R/\Lambda \to 0$, it approaches the value

$$H_{c1} = (\phi_0 / \pi R^2) \ln(R/r_c), \quad R/\Lambda \to 0 \ , \tag{33}$$

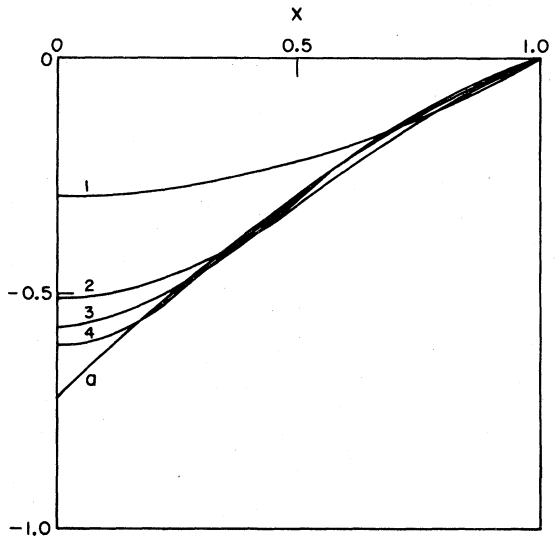

FIG. 2. Lowest-order correction to the screening function $(\Lambda/R)\hat{U}_{sc}(x)$ for $R/\Lambda \ll 1$. Curve (a) is the exact result Eq. (29); curves $M = 1, 2, 3$, and 4 are successive approximations obtained by truncating Eq. (44) at M terms.

here given in conventional units. As might be expected, the associated Larmor rotation frequency $\Omega_{c1} = e^* H_{c1}/2m^* c$ for a system of particles with charge to mass ratio e^*/m^* ($= e/m$ for Cooper pairs of electrons) is precisely the critical angular velocity[17]

$$\Omega_{c1} = (h/2\pi m^* R^2)\ln(R/r_c) \ , \tag{34}$$

for vortex formation in a rotating film of neutral superfluid with particle mass m^*. It is striking that H_{c1} varies like R^{-2} for $R \ll \Lambda$, in contrast to the approximate R^{-1} behavior[6,12,13] for large films ($R \gg \Lambda$). This latter case will be analyzed in Sec. IV.

In principle, the preceding calculation could be extended to moderate values of R/Λ by iterating the integral equation to generate the Neumann series. Unfortunately, the iterated kernels cannot be evaluated analytically, so that a more powerful approach is needed. One possibility (considered in Sec. IV) is to approximate the exact kernel $L(x,x')$ by one with the same singularity. Another more formal procedure is to expand $A(x)$ in an appropriate set of complete orthonormal functions. To generate such a set, it is convenient to reformulate the problem as a dual integral equation for the amplitude $\bar{A}(p)$ in Eq. (17). Since the superconductor extends only to $x = 1$ (in dimensionless units), it follows that the magnetic field lines can have no kinks for $x > 1$. Thus symmetry requires $h_r(x,0)$ to vanish in this region, which implies

$$-\frac{\partial}{\partial y}A(x,y)|_{y=0} = \int_0^\infty p^2 dp \bar{A}(p) J_1(px) = 0 \ , \quad x > 1 \ . \tag{35}$$

For $x < 1$, on the other hand, substitution of Eq. (17) into Eq. (6) yields

$$\int_0^\infty p dp \bar{A}(p) J_1(px)\left(p + \frac{R}{\Lambda}\right) = R/\Lambda x, \quad x < 1 \ . \tag{36}$$

In this way, the amplitude $\bar{A}(p)$ satisfies a dual integral equation[18] that has different forms for $x \gtrless 1$.

The first of these two equations can be satisfied identically with the series[19]

$$\bar{A}(p) = p^{-3/2} \sum_{m=0}^{\infty} a_m J_{2m+3/2}(p) \ . \tag{37}$$

It will simplify the notation to introduce the new coefficients

$$b_m \equiv \frac{\Gamma(m+\frac{3}{2})}{\Gamma(m+2)} \frac{a_m}{\sqrt{2}} \ , \tag{38}$$

and a lengthy analysis of Eq. (36) eventually yields an infinite set of linear equations

$$c_m b_m + \frac{R}{\Lambda} \sum_{n=0}^{\infty} d_{mn} b_n = \frac{R}{\Lambda} e_m \ . \tag{39}$$

Here

$$c_m \equiv \left[\frac{\Gamma(m+2)}{\Gamma(m+\frac{3}{2})}\right]^2 \frac{2}{3+4m} \sim \tfrac{1}{2} \text{ for } m \gg 1 \ , \tag{40}$$

and the remaining quantities are defined in terms of integrals of Jacobi polynomials[19,20] $P_m^{(1,-1/2)}(1-2x^2)$:

$$d_{mn} = d_{nm} \equiv \int_0^1 x^3 dx \, P_m P_n \ , \tag{41a}$$

$$e_m = \int_0^1 x dx \, P_m \ . \tag{41b}$$

These polynomials form a complete orthonormal set on the interval $0 \leqslant x \leqslant 1$. Alternatively (but with less motivation) the same set [Eq. (39)] of linear equations can be obtained directly from Eq. (18) by writing

$$A(x) = \sum_{m=0}^{\infty} b_m x P_m^{(1,-1/2)}(1-2x^2) \ , \tag{42}$$

and then using the orthogonality of the Jacobi polynomials. The generating function for the polynomials readily yields the value

$$e_m = \frac{1}{2m+1}\left[1 - \frac{(-1)^m \Gamma(m+\frac{1}{2})}{2\Gamma(\frac{1}{2})\Gamma(m+2)}\right] \ . \tag{43}$$

In contrast, d_{mn} does not seem expressible in closed form, but it is easily evaluated for any specific values of m and n.

Given the coefficients $\{b_m\}$, Eq. (42) allows a direct calculation of the physical quantities. In partic-

ular, the screening contribution to the total interaction is

$$\hat{U}_{sc}(x) = -\sum_{m=0}^{\infty} b_m \int_x^1 x'dx' \, P_m^{(1,-1/2)}(1-2x'^2) \ , \quad (44)$$

and the dimensionless self-energy of a single flux line therefore becomes [see Eq. (10)]

$$\hat{\epsilon} = \tfrac{1}{2} \ln\frac{R}{r_c} - \tfrac{1}{2}\sum_{m=0}^{\infty} b_m e_m \ . \quad (45)$$

In addition, Eq. (39) simplifies the magnetic moment in Eq. (12) to the expression

$$\hat{m} = \tfrac{4}{3} b_0 \ , \quad (46)$$

and the ratio $\hat{\epsilon}/\hat{m}$ then gives the exact $\hat{H}_{c1}$ for arbitrary values of R/Λ.

The preceding analysis transforms the exact integral equation to an infinite set of linear algebraic equations. Since Eq. (18) has a variational basis, it is natural to truncate these equations, keeping only the first M terms ($m = 0, 1, \ldots, M-1$) in the expansion Eq. (42). To study the convergence of this procedure, we have considered the cases $M = 1, 2, 3$, and 4, evaluating the coefficients b_m for various values of R/Λ. If $R/\Lambda \to 0$, the solution for all m is immediate

$$b_m = \frac{R}{\Lambda}\frac{e_m}{c_m}, \quad R/\Lambda \to 0 \ , \quad (47)$$

and the first four truncated approximations to $(\Lambda/R)\hat{U}_{sc}(x)$ as $R/\Lambda \to 0$ are shown in Fig. 2 for comparison with the exact first-order expression from Eq. (29). For small R/Λ, at least, the convergence appears to be good except for the region $x << 1$, where every term in Eq. (44) has zero slope, in contrast to the linear behavior of the exact expression. Figure 3 shows the approximate functions $\hat{U}_{sc}(x)$ for $R/\Lambda = 1.0$ and 10 with $M = 3$ and 4; the convergence of the series apparently worsens for large R/Λ. In principle, this procedure could be extended to include more terms, but the numerical analysis would become quite extensive. Since $\hat{\epsilon}$ involves $\hat{U}_{sc}(0)$, where the series converges most slowly, this truncation scheme is unlikely to be accurate in determining $\hat{H}_{c1}$.

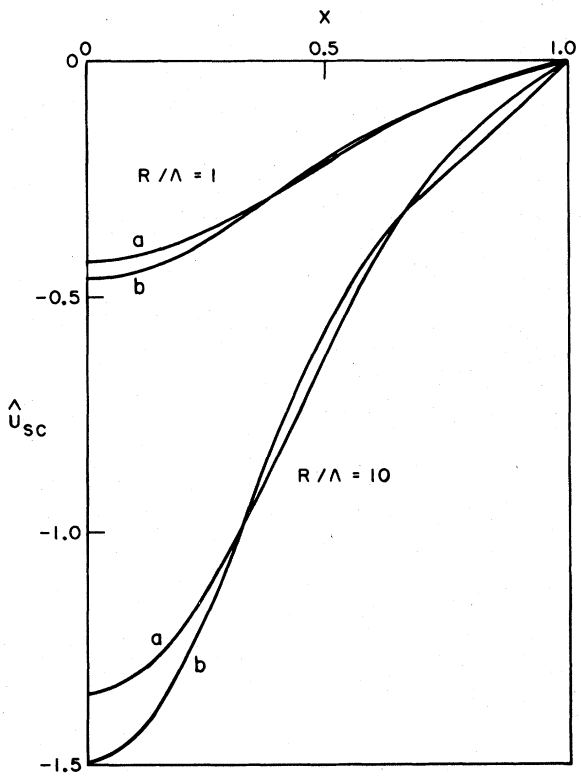

FIG. 3. $\hat{U}_{sc}(x)$ for $R/\Lambda = 1.0$ and 10, obtained by truncating Eq. (44) at 3 [curves (a)] and 4 [curves (b)] terms.

IV. APPROXIMATE SOLUTION

One common approach to integral equations is to replace the exact kernel by an approximate one that permits a complete solution of the resulting equation.[21] If desired, the difference between the approximate and exact kernels is then treated in perturbation theory. Such a technique proves extremely valuable in the present problem.

As an introduction, consider the Fourier-Bessel eigenfunctions[22]

$$\chi_n(x) = \frac{2^{1/2}}{J_0(\alpha_{1n})} J_1(\alpha_{1n}x) \ , \quad (48)$$

where α_{1n} is the nth zero of J_1. These functions are orthonormal on the interval [0,1] with weight function x according to

$$\int_0^1 xdx \, \chi_n(x)\chi_{n'}(x) = \delta_{nn'} \ . \quad (49)$$

To use them in solving Eq. (18), consider the following real symmetric kernel

$$L_0(x,x') \equiv \sum_{n=1}^{\infty} \alpha_{1n}^{-1}\chi_n(x)\chi_n(x') \ . \quad (50)$$

Since $\alpha_{1n} \sim \pi(n + \frac{1}{4})$ for large n, the discussion of Eq. (23) suggests that $L_0(x,x')$ will diverge logarithmically as $|x - x'| \to 0$, so that L_0 is a good candidate for an approximate kernel. Fortunately, the sum in Eq. (50) can be rewritten as a contour integral[22]

$$L_0(x,x') = \int_C \frac{dw}{2i}[J_1(w)Y_1(wx_>) - J_1(wx_>)Y_1(w)] \times \frac{J_1(wx_<)}{J_1(w)} \ , \quad (51)$$

where C is a contour running just to the right of the imaginary axis from $i\infty$ to $-i\infty$, and Y_n is the Neumann function.[14] If the contour is deformed far to the right, the only singularities are simple poles at the zeros of $J_1(w)$, and the sum of the residues precisely reproduces Eq. (50). Alternatively, this expression can be transformed by writing $w=\exp(\pm i\frac{1}{2}\pi)p$. A straightforward analysis gives

$$L_0(x,x')=\frac{2}{\pi}\int_0^\infty dp\left[K_1(px_>)I_1(px_<)-\frac{K_1(p)}{I_1(p)}I_1(px)I_1(px')\right] . \quad (52)$$

Comparison with Eq. (20) shows that the first term on the right-hand side is just the original kernel $L(x,x')$; hence it is convenient to rewrite Eq. (52) as

$$L(x,x')=L_0(x,x')+L_1(x,x') , \quad (53)$$

where

$$L_1(x,x')\equiv\frac{2}{\pi}\int_0^\infty dp\,\frac{K_1(p)}{I_1(p)}I_1(px)I_1(px') . \quad (54)$$

Since $L_1(x,x)$ is bounded except as $x\to 1$, it is clear that L and L_0 have the same logarithmic singularity for $|x-x'|\to 0$ almost everywhere.

Equations (50) and (53) provide an approximate solution to Eq. (18). First, solve the following integral equation for the auxiliary quantity A_0

$$A_0+(R/\Lambda)L_0A_0=(R/\Lambda)L_0g , \quad (55)$$

where

$$g(x)\equiv x^{-1} . \quad (56)$$

Here, we have introduced a matrix notation for integration over an intermediate variable, so that, for example

$$L_0g\equiv\int_0^1 x'dx'\,L_0(x,x')g(x')=\int_0^1 dx'\,L_0(x,x') . \quad (57)$$

The special form of L_0 in Eq. (50) means that $A_0(x)$ has a simple expansion in the Fourier-Bessel eigenfunctions from Eq. (48). Given A_0, the full solution A is obtained by solving a second integral equation

$$A+(R/\Lambda)L_0A+(R/\Lambda)L_1A=A_0+(R/\Lambda)L_0A_0+(R/\Lambda)L_1g , \quad (58)$$

which is better suited for approximation techniques because Tr L_1 is finite.

The solution to Eq. (55) follows directly by writing

$$A_0(x)=\sum_{n=1}^\infty C_n\chi_n(x) , \quad (59)$$

where $\{\chi_n\}$ are the eigenfunctions from Eq. (48). Substitution into Eq. (55) and use of Eqs. (49) and (50) gives the expansion coefficients

$$C_n=(1+\alpha_{1n}\Lambda/R)^{-1}\int_0^1 dx'\,\chi_n(x') , \quad (60)$$

so that

$$A_0(x)=\sum_{n=1}^\infty\chi_n(x)(1+\alpha_{1n}\Lambda/R)^{-1}\int_0^1 dx'\,\chi_n(x')=\sum_{n=1}^\infty\frac{2J_1(\alpha_{1n}x)[1-J_0(\alpha_{1n})]}{\alpha_{1n}(1+\alpha_{1n}\Lambda/R)[J_0(\alpha_{1n})]^2} . \quad (61)$$

This solution for A_0 is directly analogous to the formal one obtained for A in Eq. (24) in terms of the unknown eigenfunctions $\{\psi_n\}$. Although Eq. (61) can be rewritten as a contour integral like that in Eq. (51), the form is not particularly useful in this context and will be considered only in Sec. V.

Our basic approach is now to take A_0 as a reasonable approximation to the exact solution A. Since A_0 is well defined for all values of R/Λ, it allows us to extend the calculations of Sec. III throughout the range of values $0\leq R/\Lambda\leq\infty$. In particular, the corresponding approximate screening contribution to the interaction function Eq. (9)

$$\hat{U}_{sc0}(x)\equiv-\int_x^1 dx'\,A_0(x') , \quad (62a)$$

becomes

$$\hat{U}_{sc0}(x)=-2\sum_{n=1}^\infty\frac{[1-J_0(\alpha_{1n})][J_0(\alpha_{1n}x)-J_0(\alpha_{1n})]}{\alpha_{1n}^2(1+\alpha_{1n}\Lambda/R)[J_0(\alpha_{1n})]^2} . \quad (62b)$$

This series is easily evaluated for any particular value of R/Λ, and Fig. 4 shows the resulting function for $R/\Lambda=1.0$ and 10. The curves are qualitatively similar to those in Fig. 3, except at small x, where the present approximation should be more accurate [compare the curve (a) in Fig. 2, which is exact for small R/Λ]. Evidently, $\hat{U}_{sc0}(x)$ attains its minimum value

$$\hat{U}_{sc0}(0)=-2\sum_{n=1}^\infty\alpha_{1n}^{-2}\left[1+\alpha_{1n}\frac{\Lambda}{R}\right]^{-1}\{[J_0(\alpha_{1n})]^{-1}-1\}^2 \quad (63)$$

at the origin. Since

$$J_0(\alpha_{1n})\sim(-1)^n(2/\pi\alpha_{1n})^{1/2}$$

for $n\gg 1$, it is clear from the integral test that $\hat{U}_{sc0}(0)$ behaves like $-\ln(R/\Lambda)$ for large R/Λ. The approximate self-energy form Eq. (10) thus becomes independent of R in this limit

$$\hat{\epsilon}_0\approx\tfrac{1}{2}\ln(\Lambda/r_c), \quad R/\Lambda\gg 1 . \quad (64)$$

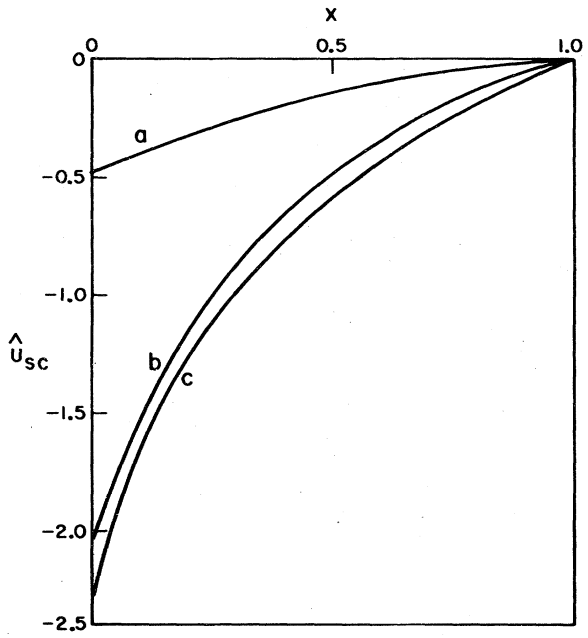

FIG. 4. Approximate screening conribution Eq. (62b) to the interaction function for $R/\Lambda = 1.0$ [curve (a)] and 10 [curve (b)]. For comparison, the screening contribution $\hat{U}_P(x) - \ln(x^{-1})$ to Pearl's solution Eq. (68) is also shown for $R/\Lambda = 10$ [curve (c)].

This limiting behavior reproduces that found by Pearl for an infinite disk ($R \to \infty$). To verify the correspondence, note that the dimensionless variable $x \equiv r/R$ in Eq. (61) becomes small as $R \to \infty$ for fixed r. The function $J_1(\alpha_{1n}x)$ then varies slowly with increasing n, and the sum in Eq. (61) can be approximated by an integral

$$A_0(r) \approx \int_\pi^\infty d\alpha \frac{J_1(\alpha r/R)}{1+\alpha\Lambda/R}\left[1-(-1)^n\left(\frac{2}{\pi\alpha}\right)^{1/2}\right] , \quad (65)$$

where the asymptotic form has been used for $J_0(\alpha_{1n})$. For $R/\Lambda \to \infty$, the change of variable $u = \alpha\Lambda/R$ leads to the simpler dimensionless expression

$$A_P(r) = \frac{R}{\Lambda}\int_0^\infty du \frac{J_1(ur/\Lambda)}{1+u}, \quad R \to \infty , \quad (66)$$

which is just that found by Pearl.[5,6] It can be evaluated explicitly to give

$$A_P(r) = \frac{R}{\Lambda}\left\{\frac{\Lambda}{r} + \frac{1}{2}\pi\left[H_{-1}\left(\frac{r}{\Lambda}\right) - Y_{-1}\left(\frac{r}{\Lambda}\right)\right]\right\} , \quad (67)$$

where H_{-1} is a Stuve function.[14] The associated dimensionless interaction function becomes

$$\hat{U}_P(r) = \tfrac{1}{2}\pi[H_0(r/\Lambda) - Y_0(r/\Lambda)] - \tfrac{1}{2}\pi[H_0(R/\Lambda) - Y_0(R/\Lambda)] , \quad (68)$$

where $\hat{U}_P$ is taken to vanish at $r = R$. This function is very similar to that obtained from the Fourier-Bessel series for large R/Λ. Figure 4 compares the screening contributions of the two solutions for $R/\Lambda = 10$.

The approximate solution $A_0(x)$ in Eq. (61) immediately provides the corresponding $\hat{H}_{c10}$ from the series Eq. (63) and the approximate magnetic moment [see Eq. (12b)]

$$\hat{m}_0 = \pi\sum_{n=1}^{\infty}\frac{1}{\alpha_{1n}(1+\alpha_{1n}\Lambda/R)}\left[1-\frac{1}{J_0(\alpha_{1n})}\right] . \quad (69)$$

The integral test again shows that $\hat{m}_0$ behaves like $\ln(R/\Lambda)$ for large R/Λ, in contrast to Pearl's prediction[6,12,13] $\hat{m}_P \approx \frac{1}{2}\pi$ based on Eq. (67). Note, however, that the integral Eq. (11) weights most heavily the outer part of the disk, which is the region where the exact solution differs most from that for an infinite plane. Thus it is not obvious that A_P can correctly predict the value of $\hat{m}$, even for large R/Λ, and this discrepancy remains unresolved.

The two series Eqs. (63) and (69) have been evaluated numerically to give the dimensionless lower critical field $\hat{H}_{c10}$ shown in Fig. 5 for $R/r_c = 10^5$. If $R = 10^{-1}$ cm, for example, the predicted values for $\Lambda = 10^{-2}$, 10^{-1}, and 1 cm, are 1.8×10^{-4}, 8.7×10^{-5}, and 7.5×10^{-5} G, respectively. Conceivably, observation of H_{c1} could provide a direct measure of the effective penetration depth Λ. Pearl's picture of flux penetration in thin films has had only partial experimental verification[23] so that this possibility is especially interesting.

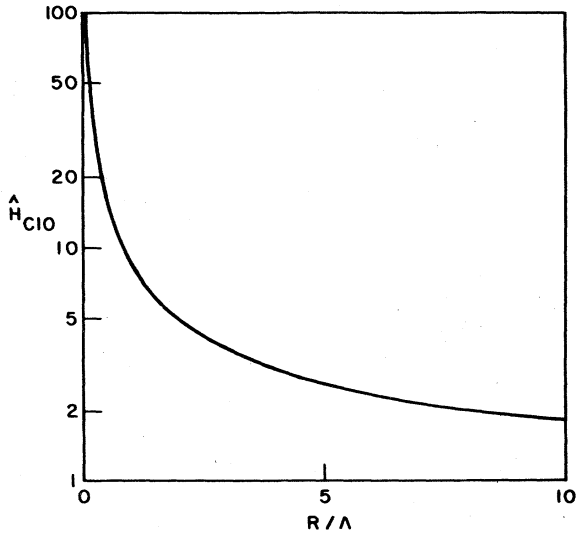

FIG. 5. Dimensionless lower critical field $\hat{H}_{c10}$ evaluated from Eqs. (10b), (13b), (63), and (69) for $R/r_c = 10^5$.

The preceding analysis depends on the approximation of neglecting the kernel L_1 in Eqs. (58), thereby replacing the exact $A(x)$ by the solution $A_0(x)$ to Eq. (55). To investigate the effect of L_1, it is convenient first to rewrite Eq. (58) as

$$A+\tilde{L}A=A_0+\tilde{L}g \ , \tag{70}$$

where

$$\tilde{L}\equiv[1+(R/\Lambda)L_0]^{-1}(R/\Lambda)L_1 \ . \tag{71}$$

Although we are most interested in the behavior for large R/Λ, it is not, in general, permissible to take this limit directly. Nevertheless, the new kernel $\tilde{L}$ behaves better as $R/\Lambda\to\infty$ than does the original one [$(R/\Lambda)L$ in Eq. (18)]. Indeed, $\tilde{L}$ now has a finite trace, and a perturbation expansion of Eq. (70) should converge for $\mathrm{Tr}\tilde{L}<1$. To study the dependence of $\mathrm{Tr}\tilde{L}$ on R/Λ, we diagonalize the operator $[1+(R/\Lambda)L_0]^{-1}$ with the eigenfunctions from Eq. (48) to obtain

$$\mathrm{Tr}\tilde{L}=\sum_{n=1}^{\infty}\left(1+\frac{R}{\Lambda\alpha_{1n}}\right)^{-1}\left(\frac{R}{\Lambda}\right)(L_1)_{nn} \ , \tag{72}$$

where

$$(L_1)_{mn}=\int\int_0^1 x\,dx\,x'\,dx'\,\chi_m(x)L_1(x,x')\chi_n(x') \ . \tag{73}$$

Use of Eq. (54) and standard formulas yields the exact expression

$$(L_1)_{mn}=\frac{4}{\pi}\alpha_{1m}\alpha_{1n}\int_0^{\infty}dp\,\frac{K_1(p)I_1(p)}{(p^2+\alpha_{1m}^2)(p^2+\alpha_{1n}^2)} \ . \tag{74}$$

To make further progress, note that

$$2K_1(p)I_1(p)\approx\begin{cases}1, & p\ll 1\\ p^{-1}, & p\gg 1,\end{cases} \tag{75}$$

and it is therefore natural to introduce the approximation

$$2K_1(p)I_1(p)\approx(1+p)^{-1} \ . \tag{76}$$

The resulting approximate integral is easily evaluated to give

$$(L_1)_{mn}\approx\frac{\alpha_{1m}\alpha_{1n}}{\alpha_{1n}^2-\alpha_{1m}^2}\left(\frac{2\pi^{-1}\ln\alpha_{1m}+\alpha_{1m}^{-1}}{1+\alpha_{1m}^2}-\frac{2\pi^{-1}\ln\alpha_{1n}+\alpha_{1n}^{-1}}{1+\alpha_{1n}^2}\right) \ , \tag{77}$$

and $(L_1)_{nn}$ follows with l'Hôpital's rule. The integral test for convergence indicates that $\mathrm{Tr}\tilde{L}$ is of order $(\ln R/\Lambda)^2$ as $R/\Lambda\to\infty$, and numerical evaluation shows that $\mathrm{Tr}\tilde{L}<1$ for $R/\Lambda<18.6$ (see Fig. 6). This behavior is to be contrasted with that discussed below Eq. (26), where $(R/\Lambda)\,(\mathrm{Tr}L^2)^{1/2}<1$ only for $R/\Lambda<2.05$.

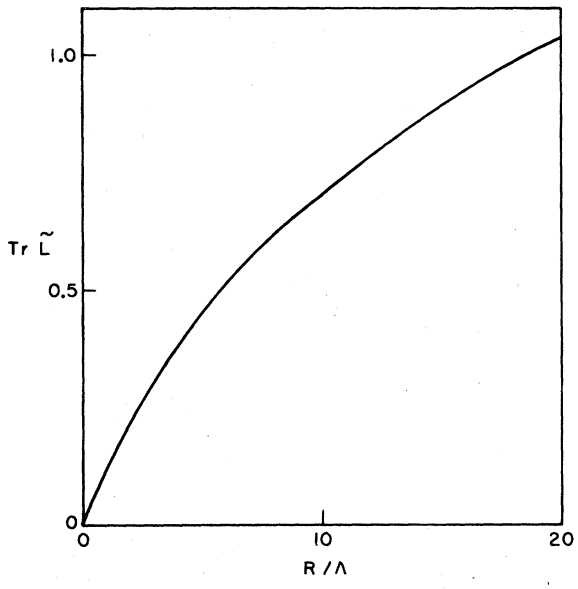

FIG. 6. Quantity $\mathrm{Tr}\tilde{L}$ from Eqs. (72) and (77), as a function of R/Λ.

The Neumann solution to Eq. (70) takes the form

$$\begin{aligned}A&=A_0+\tilde{L}(g-A_0)+\cdots\\&=A_0+[1+(R/\Lambda)L_0]^{-1}(R/\Lambda)L_1\\&\quad\times[1+(R/\Lambda)L_0]^{-1}g+\cdots \ ,\end{aligned} \tag{78}$$

where we have used Eq. (55) in obtaining the second form. The complete set of Fourier-Bessel eigenfunctions from Eqs. (48)–(50) gives the first correction

$$A(x)-A_0(x)\approx\sum_{mn=1}^{\infty}\frac{(R/\Lambda)(L_1)_{mn}}{(1+R/\Lambda\alpha_{1m})(1+R/\Lambda\alpha_{1n})}\times\chi_m(x)\int_0^1 dx'\,\chi_n(x') \ . \tag{79}$$

Substitution into Eq. (9), for example, provides the approximate correction to the self-energy of a single flux line

$$\hat{U}_{\mathrm{sc}}(0)-\hat{U}_{\mathrm{sc0}}(0)\approx-2\sum_{mn=1}^{\infty}\left(1-\frac{1}{J_0(\alpha_{1m})}\right)\left(1-\frac{1}{J_0(\alpha_{1n})}\right)\times\frac{(R/\Lambda)(L_1)_{mn}}{(\alpha_{1m}+R/\Lambda)(\alpha_{1n}+R/\Lambda)} \ . \tag{80}$$

If the summation is replaced by a double integral and the oscillating contributions from $J_0(\alpha_{1m})$ and $J_0(\alpha_{1n})$ are neglected, use of Eq. (77) shows that the right-hand side of Eq. (80) is small, of order (Λ/R)

$(\ln R/\Lambda)^2$ for large R/Λ. In contrast, the correction to $\hat{m}-\hat{m}_0$ behaves quite differently in the same limit. Equation (12b) gives

$$\hat{m}-\hat{m}_0=-\frac{1}{2}\pi\frac{R}{\Lambda}\int_0^1 x^2dx\,[A(x)-A_0(x)]$$
$$\approx-\pi\sum_{mn=1}^{\infty}\left[1-\frac{1}{J_0(\alpha_{1n})}\right]\times\frac{(R/\Lambda)^2(L_1)_{mn}}{(\alpha_{1m}+R/\Lambda)(\alpha_{1n}+R/\Lambda)}\ . \quad (81)$$

This double summation has essentially the same structure as that in Eq. (80), and $\hat{m}-\hat{m}_0$ therefore diverges like $(\ln R/\Lambda)^2$ for $R/\Lambda\to\infty$. We conclude that A_0 cannot be considered a good approximation for all R/Λ, although Fig. 6 indicates that it is probably reasonable for $R/\Lambda\lesssim 20$. Since Pearl's solution is likely to describe the regime $R/\Lambda\gtrsim 10$, we believe that A_0 suffices in most cases of practical interest.

V. FLUX LINES IN ARBITRARY POSITIONS

In an infinite film, the interaction between two flux lines depends only on their relative separation, but the situation is more complicated in a finite disk. To study this case, it is essential to return to the original Eq. (3). We first generalize the phase function $S(r,\theta)$ to describe a single flux line located at the point (r_0,θ_0). In the gauge $\vec{\nabla}\cdot\vec{A}=0$, Eq. (2) requires that S satisfy Laplace's equation. Furthermore, the two terms in Eq. (2) represent distinct physical contributions to $\vec{j}$, and each must produce zero net flow through the boundary

$$\hat{r}\cdot\vec{\nabla}S=0 \quad \text{at } r=R\ , \quad (82a)$$

$$\hat{r}\cdot\vec{A}=0 \quad \text{at } r=R\ . \quad (82b)$$

As is familiar from the hydrodynamics of ideal classical fluids in cylindrical containers,[24] the necessary function $S(\vec{r},\vec{r}_0)$ follows from the method of images as the real part of the complex potential

$$S(\vec{r},\vec{r}_0)=\mathrm{Re}F(z,z_0)\ , \quad (83a)$$

with

$$F(z,z_0)=-i\ln\left[\frac{R}{r_0}\left(\frac{z-z_0}{z-\bar{z}_0}\right)\right]\ . \quad (83b)$$

Here, $z=r\exp(i\theta)$, $z_0=r_0\exp(i\theta_0)$, and $\bar{z}_0=(R^2/r_0)\exp(i\theta_0)$. In addition, the imaginary part is the stream function

$$\Psi=\mathrm{Im}F=\tfrac{1}{2}\ln\left[\frac{1-2xx_0\cos(\theta-\theta_0)+x^2x_0^2}{x^2-2xx_0\cos(\theta-\theta_0)+x_0^2}\right]\ , \quad (84)$$

where, as previously, $x=r/R$ and $x_0=r_0/R$. The Cauchy-Riemann equations may be written

$$\vec{\nabla}S=\vec{\nabla}\Psi\times\hat{z}\ , \quad (85)$$

and Eq. (82a) holds identically because Ψ vanishes for $x=1$.

Since the vector potential has the form $\vec{A}=A_r\hat{r}+A_\theta\hat{\theta}$, the same dimensionless variables as in Eq. (6) reduce the two components of Eq. (3) to

$$\Delta A_r-x^{-2}A_r-2x^{-2}\frac{\partial A_\theta}{\partial\theta}=\frac{2R}{\Lambda}\delta(y)\left[A_r-\frac{1}{x}\frac{\partial\Psi}{\partial\theta}\right]\eta(1-x)\ , \quad (86a)$$

$$\Delta A_\theta-x^{-2}A_\theta+2x^{-2}\frac{\partial A_r}{\partial\theta}=\frac{2R}{\Lambda}\delta(y)\left[A_\theta+\frac{\partial\Psi}{\partial x}\right]\eta(1-x)\ . \quad (86b)$$

Here $\eta(x)$ again denotes the unit step function, Δ is the Laplacian in cylindrical coordinates (x,θ,y), and the Cauchy-Riemann equations have been used. In addition, the gauge condition requires

$$\frac{1}{x}\frac{\partial}{\partial x}(xA_r)+\frac{1}{x}\frac{\partial}{\partial\theta}A_\theta=0\ . \quad (87)$$

It is convenient to write $A_r=x^{-1}B$ and $A_\theta=A$, and then to expand all quantities in Fourier series

$$A_r=x^{-1}B=\sum_m{}'\,x^{-1}B^{(m)}e^{im\theta}\ , \quad (88a)$$

$$A_\theta=A=\sum_m{}'\,A^{(m)}e^{im\theta}+A^{(0)}\ , \quad (88b)$$

$$\Psi=\sum_m{}'\,\Psi^{(m)}e^{im\theta}+\Psi^{(0)}\ . \quad (88c)$$

Here the prime means to omit the term $m=0$, and the contribution $B^{(0)}$ may be neglected since it is simply a constant. The Fourier coefficients in Eq. (88c) follow by expanding the logarithm in Eq. (83b) in a Taylor series to give

$$\Psi^{(0)}(x,x_0)=-\ln x_>\ , \quad (89a)$$

$$\Psi^{(m)}(x,x_0)=\frac{1}{2|m|}\left[\left(\frac{x_<}{x_>}\right)^{|m|}-(xx_0)^{|m|}\right]e^{-im\theta_0},\quad m\neq 0\ , \quad (89b)$$

where $x_<$ and $x_>$ are the smaller and larger of x and x_0. The gauge condition Eq. (87) becomes

$$A^{(m)}=\frac{i}{m}\frac{\partial B^{(m)}}{\partial x},\quad m\neq 0\ , \quad (90)$$

and the other two equations can be manipulated to give

$$\left[\frac{\partial^2}{\partial x^2}+\frac{1}{x}\frac{\partial}{\partial x}-\frac{1}{x^2}+\frac{\partial^2}{\partial y^2}\right]A^{(0)} = \frac{2R}{\Lambda}\delta(y)\left[A^{(0)}-\frac{1}{x}\eta(x-x_0)\right]\eta(1-x) \ , \quad (91a)$$

$$\left[\frac{\partial^2}{\partial x^2}+\frac{1}{x}\frac{\partial}{\partial x}-\frac{m^2}{x^2}+\frac{\partial^2}{\partial y^2}\right]B^{(m)} = \frac{2R}{\Lambda}\delta(y)\left[B^{(m)}-im\Psi^{(m)}\right]\eta(1-x) \ , \quad (91b)$$

for $m=0$ and $m\neq 0$, respectively.

As in Sec. II, the most interesting physical quantities can be expressed directly in terms of the functions $A^{(0)}$ and $B^{(m)}$. Suppose that there is a flux line at $\vec{x}_0$. Integrating the Lorentz force from the edge of the disk to some final point $\vec{x}$ easily gives the dimensionless interaction energy $\hat{U}(\vec{x},\vec{x}_0)$ between two flux lines at $\vec{x}$ and $\vec{x}_0$. Since Eq. (2) distinguishes between the unscreened vortex currents and the induced screening currents, the corresponding interaction function will be written as the sum of two physically distinct terms

$$\hat{U}(\vec{x},\vec{x}_0)=\hat{U}_v(\vec{x},\vec{x}_0)+\hat{U}_{sc}(\vec{x},\vec{x}_0) \ . \quad (92)$$

A straightforward calculation yields [see Eq. (84)]

$$\hat{U}_v(\vec{x},\vec{x}_0)=\Psi(\vec{x},\vec{x}_0) \ , \quad (93a)$$

$$U_{sc}(\vec{x},\vec{x}_0)=-\int_x^1 dx' A^{(0)}(x',x_0) + \sum_m{}' im^{-1}e^{im\theta}B^{(m)}(x,\vec{x}_0) \ , \quad (93b)$$

where we have used the boundary condition $B^{(m)}=0$ at $x=1$. The term $\hat{U}_v$ is the interaction energy of two vortices in a neutral superfluid film confined to a circle of radius R, because the screening contribution becomes negligible when $\Lambda >> R$. Note that U_v has the expected logarithmic dependence ($\propto -\ln|\vec{x}-\vec{x}_0|$) for small separations, but only if $|\vec{x}-\vec{x}_0|$ is much less that the smaller of $1-x$ and $1-x_0$. Otherwise, the image vortices at $\hat{x}/x$ or $\hat{x}_0/x_0$ predominate, and $\hat{U}_v$ in fact vanishes if x or $x_0=1$. Thus the presence of boundaries alters the interaction function significantly because of the long-range interaction in a neutral superfluid.

In a similar way, it is not difficult to show that the total free energy of an assembly of flux lines at $\{\vec{x}_k\}$ becomes

$$F=(\phi_0^2/4\pi^2\Lambda)\hat{F} \ , \quad (94a)$$

where

$$\hat{F}=\sum_k \epsilon(\vec{x}_k)+\tfrac{1}{2}\sum_{kl}{}'\hat{U}(\vec{x}_k,\vec{x}_l) \ , \quad (94b)$$

and

$$\epsilon(\vec{x}_k)=\tfrac{1}{2}\ln(R/r_c)+\tfrac{1}{2}\ln(1-x_k^2)+\tfrac{1}{2}\hat{U}_{sc}(\vec{x}_k,\vec{x}_k) \quad (94c)$$

is the self-energy of a single flux line at $\vec{x}_k$ [compare Eq. (10b)]. Finally, the total magnetic moment Eq. (11) for the system is

$$\hat{m}=\sum_k \hat{m}(x_k) \ , \quad (95a)$$

where

$$\hat{m}(x_k)=\tfrac{1}{2}\pi\frac{R}{\Lambda}\int_0^1 x'dx'\left[\eta(x'-x_k)-x'A^{(0)}(x',x_k)\right] \ . \quad (95b)$$

Before discussing the detailed form of $U(\vec{x},\vec{x}_0)$, we demonstrate the following theorem: In an applied field H corresponding to many flux lines with nonoverlapping cores ($H_{c1}<<H<<H_{c2}$), the equilibrium configuration for arbitrary R/Λ has a *constant flux density, independent of the presence of boundaries.* The proof starts from the dimensionless Gibbs free energy

$$\hat{G}=\hat{F}-\hat{H}\hat{m} \quad (96)$$

and replaces the sum over discrete flux lines by an integration over an axisymmetric continuous surface density $\hat{n}(x)$

$$\hat{G}\approx\tfrac{1}{2}\int\int d^2x\,d^2x'\,\hat{n}(x)\hat{n}(x')\hat{U}(\vec{x},\vec{x}') - \hat{H}\int d^2x\,\hat{n}(x)\hat{m}(x) \ . \quad (97)$$

Here, we have omitted the self-energy contribution and therefore neglect corrections of order H/H_{c1}. The angular integrals can be performed explicitly [see Eqs. (89a), (93b), and (95b)] to give

$$\hat{G}=2\pi^2\int\int_0^1 xdxx'\,dx'\,\hat{n}(x)\hat{n}(x') \times\left[\ln(1/x_>)-\int_x^1 dy\,A^{(0)}(y,x')\right] - \frac{\pi^2R\hat{H}}{\Lambda}\int\int_0^1 xdxx'\,dx'\,\hat{n}(x) \times\left[\eta(x'-x)-x'A^{(0)}(x',x)\right] \ , \quad (98)$$

where only the azimuthally symmetric contributions appear. In fixed applied field $\hat{H}$, the equilibrium condition $\delta G/\delta n(x)=0$ leads to an integral equation

$$\int_0^1 x'dx'\left[\ln(1/x_>)-\int_x^1 dy\,A^{(0)}(y,x')\right]\hat{n}(x') = \frac{R\hat{H}}{4\Lambda}\int_0^1 (x')^2dx'\left[\eta(x'-x)/x'-A^{(0)}(x',x)\right] \ , \quad (99)$$

whose solution is the equilibrium flux-line distribution $\hat{n}(x)$.

This equation looks daunting, but special properties of $A^{(0)}$ ensure that a constant density is the only solution. To verify this assertion, note that the integral equation for $A^{(0)}(x,x')$ differs from Eq. (18) only in that the integral on the right-hand side runs from x' to 1, instead of 0 to 1 [compare Eqs. (6) and (91a)]. Consideration of the corresponding Neumann expansion for $A^{(0)}$ shows that the quantity in brackets on the right-hand side of Eq. (99) has the form.

$$\frac{1}{x'}\eta(x'-x)-A^{(0)}(x',x)=\int_x^1 dy\, f(x',y) \ , \qquad (100)$$

where $f(x',y)$ is a *symmetric* function of its arguments. A little manipulation then transforms Eq. (99) into the more transparent equation

$$\int_x^1 dy \int_0^1 dz\, f(y,z)\left[\int_0^z x'dx'\hat{n}(x')-\frac{R\hat{H}z^2}{4\Lambda}\right] \ . \qquad (101)$$

It is evident by inspection that

$$\hat{n}(x)=R\hat{H}/2\Lambda(=\text{const}) \qquad (102)$$

is an exact solution of Eq. (101). To prove that it is also unique, we expand $A^{(0)}(x,x')$ in the complete set of eigenfunctions $\{\psi_n(x)\}$ from Eq. (22). A straightforward calculation shows that the symmetric function $f(y,z)$ defined in Eq. (100) is given by

$$f(y,z)=\sum_{n=1}^{\infty}\psi_n(y)(1+R/\Lambda l_n)^{-1}\psi_n(z) \ . \qquad (103)$$

Differentiate Eq. (101) with respect to x and combine with Eq. (103). The assumed completeness of $\{\psi_n\}$ immediately implies that

$$\int_0^1 zdz\,\psi_n(z)\left[z^{-1}\int_0^z x'dx'\,\hat{n}(x')-\left[\frac{R\hat{H}}{4\Lambda}\right]z\right]=0 \qquad (104)$$

for all n. As a result, the areal density $\hat{n}(x)$ in fact satisfies the simpler integral equation

$$\int_0^z x'dx'\,\hat{n}(x')=\left[\frac{R\hat{H}}{4\Lambda}\right]z^2 \ . \qquad (105)$$

Differentiation with respect to z reproduces the constant solution Eq. (102). In more familiar dimensional variables, it has the expected value

$$n=\hat{n}/R^2=H/\phi_0 \ . \qquad (106)$$

Thus the magnetic flux density B is just equal to H in the regime $H_{c1}\ll H\ll H_{c2}$, apart from corrections of order H_{c1}/H.[25]

The conclusion that the flux lines assume a constant density in the regime $H_{c1}\ll H\ll H_{c2}$ is plausible but not self-evident because of the presence of boundaries. For example, the equilibrium distribution of electrostatic charge on a conducting disk peaks sharply at the outer edge.[26] Here, in contrast, the flux lines act like an incompressible medium.[25] An earlier investigation[27] of rectilinear vortices in a bulk rotating neutral superfluid had obtained this same uniform distribution for an arbitrary multiply connected domain, but the analysis depended crucially on the properties of harmonic functions and the Green's function for Poisson's equation. Here, in contrast, the superconducting screening currents complicate the problem, and the proof of a constant flux density for a superconducting disk with arbitrary value of R/Λ appears to be new. Previously, Maki[12] reached a similar conclusion based on an integral equation whose kernel differed from that in Eq. (99) owing to the neglect of the boundaries and associated image effects. Thus his inferred constant flux density was only an approximate solution to the corresponding integral equation.

The preceding study is independent of the detailed form of the induced screening currents, and it is now interesting to consider this latter question. A Hankel transform can reduce each of the partial differential equations (91) to Fredholm integral equations analogous to Eq. (18), but they have no obvious analytical solutions. Instead, we rely on the same approximation used in Sec. IV. It is somewhat simpler to proceed directly by expanding $B^{(m)}$ in a Fourier-Bessel series

$$B^{(m)}=\sum_{n=1}^{\infty}F_n^{(m)}(y)\chi_n^{(m)}(x) \ , \qquad (107a)$$

where

$$\chi_n^{(m)}(x)\equiv\frac{2^{1/2}J_{|m|}(\alpha_{mn}x)}{J_{|m|-1}(\alpha_{mn})} \qquad (107b)$$

is a set of orthonormal eigenfunctions, and α_{mn} is the nth zero of J_m. Substitution into Eq. (91b) for $x<1$ shows that $F_n^{(m)}(y)$ is proportional to $\exp(-\alpha_{mn}|y|)$. Use of the discontinuity condition on the vertical gradient at $y=0$ and recursion relations for Bessel functions yields the approximate solution in the plane of the disk

$$B^{(m)}(x,\vec{x}_0)=\sum_{n=1}^{\infty}\frac{ime^{-im\theta_0}\chi_n^{(m)}(x)\chi_n^{(m)}(x_0)}{\alpha_{mn}^2(1+\alpha_{mn}\Lambda/R)} \ . \qquad (108a)$$

Similarly, Eq. (91a) has the approximate Fourier-Bessel solution [compare Eq. (61)]

$$A^{(0)}(x,x_0)=2\sum_{n=1}^{\infty}\frac{J_1(\alpha_{1n}x)[J_0(\alpha_{1n}x_0)-J_0(\alpha_{1n})]}{\alpha_{1n}(1+\alpha_{1n}\Lambda/R)[J_0(\alpha_{1n})]^2} \ . \qquad (108b)$$

The approximate screening contribution to the interaction function now follows by substituting Eqs. (108) into Eq. (93b). Evaluating the integrals explicitly, we find

$$\hat{U}_{sc0}(x,x',\theta-\theta') = -2\sum_{n=1}^{\infty}\frac{[J_0(\alpha_{1n}x)-J_0(\alpha_{1n})][J_0(\alpha_{1n}x')-J_0(\alpha_{1n})]}{\alpha_{1n}^2(1+\alpha_{1n}\Lambda/R)[J_0(\alpha_{1n})]^2} - \sum_m{}' \sum_{n=1}^{\infty} e^{im(\theta-\theta')}\frac{\chi_n^{(m)}(x)\chi_n^{(m)}(x')}{\alpha_{mn}^2(1+\alpha_{mn}\Lambda/R)} , \tag{109}$$

which manifestly vanishes as $R/\Lambda \to 0$. If either x or $x' \to 0$, this expression correctly reproduces the approximation Eq. (62b) for a flux line at the center of the disk.

The presence of nearby boundaries greatly complicates the interaction function, even in the simplest case [compare Eqs. (84) and (93a)] of a neutral superfluid without screening currents. Nevertheless, the approximate total interaction $\hat{U}_0 \equiv \hat{U}_v + \hat{U}_{sc0}$ also correctly reproduces Pearl's solution Eq. (68) for fixed $\vec{r}$ and $\vec{r}'$ as $R/\Lambda \to \infty$. It is first convenient to rewrite $\hat{U}_v$ in Eq. (93a) as a Fourier-Bessel series; an elementary calculation shows that the total interaction $\hat{U}_0$ has the same form as in Eq. (109) except that $\alpha(\alpha + R/\Lambda)$ replaces $-\alpha^2(1+\alpha\Lambda/R)$ in the denominators. The sums over n can then be expressed as contour integrals that run just to the right of the imaginary axis; as in Eq. (51), writing out the integrals explicitly gives the equivalent representation

$$U_0(\vec{r},\vec{r}') = \frac{\phi_0^2}{2\pi^3\Lambda}\int_0^{\infty}\frac{du}{1+u^2}\left[K_0\left(\frac{u}{\Lambda}|\vec{r}-\vec{r}'|\right) - \frac{I_0(ur/\Lambda)I_0(ur'/\Lambda)K_0(uR/\Lambda)}{I_0(uR/\Lambda)} + \frac{[I_0(uR/\Lambda)-I_0(ur/\Lambda)][I_0(uR/\Lambda)-I_0(ur'/\Lambda)]}{(uR/\Lambda)I_1(uR/\Lambda)I_0(uR/\Lambda)} - \sum_m{}' e^{im(\theta-\theta')}\frac{I_m(ur/\Lambda)I_m(ur'/\Lambda)K_m(uR/\Lambda)}{I_m(uR/\Lambda)}\right] , \tag{110}$$

where we have now reverted to the usual dimensional variables. Only the first term in the integrand is independent of R/Λ, so that all the remaining contributions reflect the presence of boundaries. In general, these latter terms have no simple interpretation as the effect of discrete images. If $R/\Lambda \to 0$, however, it is not difficult to verify that Eq. (110) reproduces Eq. (93a) for a neutral superfluid, with the sum on $m \neq 0$ constituting the effect of the pair of image vortices. In the opposite limit ($R/\Lambda \to \infty$ for fixed $\vec{r}$ and $\vec{r}'$), only the first term of the integrand contributes, giving Pearl's result [compare Eq. (68)]

$$\lim_{R/\Lambda\to\infty} U_0(\vec{r},\vec{r}') = \frac{\phi_0^2}{2\pi^3\Lambda}\int_0^{\infty}\frac{du}{1+u^2}K_0\left(\frac{u}{\Lambda}|\vec{r}-\vec{r}'|\right) = \frac{\phi_0^2}{8\pi\Lambda}\left[H_0\left(\frac{|\vec{r}-\vec{r}'|}{\Lambda}\right) - Y_0\left(\frac{|\vec{r}-\vec{r}'|}{\Lambda}\right)\right] . \tag{111}$$

As expected, this limit restores translational invariance. For small $|\vec{r}-\vec{r}'|$, Eq. (111) exhibits the same logarithmic behavior as Eq. (93a) for a neutral superfluid, but the screening currents become effective with increasing separation, and Eq. (111) eventually decreases like $\phi_0^2/4\pi^2|\vec{r}-\vec{r}'|$ for $|\vec{r}-\vec{r}'|/\Lambda \gg 1$.

VI. DISCUSSION

The present work has studied the behavior of flux lines in a thin superconducting disk of radius R. Since the equations are linear, it is sufficient to investigate the structure of a single flux line, for the interaction between pairs then follows directly from the Lorentz force. Although this connection between the current around one line and the pair interaction may at first seem surprising, it has a direct analog in electrostatics, where the potential and electric field of a single test charge in the presence of arbitrary fixed conductors also determines the interaction energy of an assembly of charges.

The presence of boundaries greatly complicates the problem, and it has not proved possible to obtain an exact solution, even for a single flux line at the center of the disk. We have, however, constructed an approximate solution Eq. (61) that has the correct limiting behavior both for large and small values of R/Λ. In the former case, it reproduces Pearl's results,[5,6] and in the latter, it reduces to that for a neutral superfluid. Thus it provides a convenient in-

terpolation formula that remains well defined even for $R/\Lambda \to \infty$. In contrast, a naive perturbation solution of Eq. (18) in powers of R/Λ is bound to fail for sufficiently large values (in practice, probably around $R \approx 2\Lambda$). Our approximate solution determines a variety of physical quantities, such as the lower critical field for flux penetration in the disk. Direct measurement of H_{c1} would be very interesting, for it would help verify Pearl's original calculations.

Recent theories of two-dimensional systems have stimulated interest in thin superconducting films.[1-4] To the extent that the interaction between flux lines is purely logarithmic, the Kosterlitz-Thouless description and its generalizations apply directly. Such a situation cannot hold in a large disk ($R >> \Lambda$), for the interactions then behave predominantly like r_{ij}^{-1}. If $R << \Lambda$, however, the interactions indeed become logarithmic, but it is not clear how the presence of boundaries affects the predictions of the theory. Even for neutral vortices in thin superfluid films, the interactions deviate from $\ln r_{ij}$ as soon as r_{ij} is some finite fraction of the radius R [see Eq. (93a)], or when either $\vec{r}_i$ or $\vec{r}_j$ approaches the edge. Thus the interaction function Eq. (111) contains important nonlogarithmic contributions for arbitrary values of R/Λ. In this context, the distinction between an infinite superconducting disk and a bounded neutral superfluid film is largely one of detail. Such a viewpoint raises the interesting question whether any interaction function that is logarithmic at short distances will lead to the Kosterlitz-Thouless phenomena.

It is also interesting to consider thin films with other geometries, for example a long strip of width $2a$. The energy barrier for a flux line to cross this strip[1] depends on the ratio a/Λ, as will the response to an applied transport current. These questions merit further investigation.

ACKNOWLEDGMENTS

I am grateful to M. R. Beasley, A. T. Fiory, D. S. Fisher, A. F. Hebard, B. Å. Huberman, and S. A. Trugman for helpful discussions and comments, and to the National Science Foundation for partial support under Grant No. NSF DMR 78-25258.

[1]M. R. Beasley, J. E. Mooij, and T. P. Orlando, Phys. Rev. Lett. 42, 1165 (1979).
[2]S. Doniach and B. A. Huberman, Phys. Rev. Lett. 42, 1169 (1979); B. A. Huberman and S. Doniach, Phys. Rev. Lett. 43, 950 (1979).
[3]B. I. Halperin and D. R. Nelson, J. Low Temp. Phys. 36, 599 (1979).
[4]L. A. Turkevich, J. Phys. C 12, L385 (1979).
[5]J. Pearl, in *Low Temperature Physics–LT9,* edited by J. G. Daunt, D. O. Edwards, F. J. Milford, and M. Yaqub (Plenum, New York, 1965), Part A, p. 566; Appl. Phys. Lett. 5, 65 (1964).
[6]J. Pearl, thesis (Polytechnic Institute of Brooklyn, 1965) (unpublished).
[7]V. L. Berezinskii, Sov. Phys. JETP 34, 610 (1972).
[8]J. M. Kosterlitz and D. J. Thouless, J. Phys. C 5, L124 (1972); 6, 1181 (1973); *Progress in Low Temperature Physics,* edited by D. F. Brewer (North-Holland, Amsterdam, 1978), Vol. VIIB, p. 371.
[9]V. N. Popov, Sov. Phys. JETP 37, 341 (1973).
[10]J. M. Kosterlitz, J. Phys. C 7, 1046 (1974).
[11]D. R. Nelson and J. M. Kosterlitz, Phys. Rev. Lett. 39, 1201 (1977).
[12]K. Maki, Ann. Phys. (N.Y.) 34, 363 (1965).
[13]A. L. Fetter and P. C. Hohenberg, Phys. Rev. 159, 330 (1967).
[14]The notation is that of *Handbook of Mathematical Functions,* edited by M. Abramowitz and I. A. Stegun (Natl. Bur. Stand., Washington, D.C., 1968), Chaps. 9–12.
[15]F. Smithies, *Integral Equations* (Cambridge University Press, Cambridge, 1962), Chaps. I, VI, and VII.
[16]I. S. Gradshteyn and I. M. Ryzhik, *Table of Integrals, Series, and Products* (Academic, New York, 1965), Secs. 5.11, 6.574, 8.11, and 9.13.
[17]W. F. Vinen, Nature 181, 1524 (1958).
[18]This equation was derived independently by S. A. Trugman (private communication).
[19]C. J. Tranter, *Integral Transforms in Mathematical Physics,* 3rd ed. (Methuen, London, 1966), Chap. VIII.
[20]The notation is that of Ref. 14, Chap. 22, which differs from that of Ref. 19.
[21]G. F. Carrier, M. Krook, and C. E. Pearson, *Functions of a Complex Variable* (McGraw-Hill, New York, 1966), Chap. 8.
[22]G. N. Watson, *A Treatise on the Theory of Bessel Functions,* 2nd ed. (Cambridge University Press, Cambridge, 1966), Chap. XVIII.
[23]A. T. Fiory, Phys. Rev. B 8, 5039 (1973).
[24]L. M. Milne-Thomson, *Theoretical Hydrodynamics,* 5th ed. (MacMillan, London, 1968), Chap. 13.
[25]E. Conen and A. Schmid, J. Low Temp. Phys. 17, 331 (1974).
[26]J. D. Jackson, *Classical Electrodynamics* (Wiley, New York, 1962), Sec. 3.12.
[27]A. L. Fetter, Phys. Rev. 152, 183 (1966).